

Magnetically Levitated Conveyor Using High T_c Superconducting Magnetic Bearings (SMBs) and Its Dynamic Characteristics

Bumpei NAKAYA
Kyushu Institute of Technology
Kitakyushu, Fukuoka 804-8550, Japan

Mochimitsu KOMORI*
Kyushu Institute of Technology
Kitakyushu, Fukuoka 804-8550, Japan

Ken-ichi ASAMI
Kyushu Institute of Technology
Kitakyushu, Fukuoka 804-8550, Japan

Nobuo SAKAI
Kyushu Institute of Technology
Kitakyushu, Fukuoka 804-8550, Japan

Abstract

Our group has developed a new conveyor using superconducting levitation. The conveyor is composed of a levitated table and a conveying table. The gap between levitated table and conveying table is detected by using a Hall sensor on the superconductor. The position of the table is controlled by using the PD control. In this paper we discuss a superconducting magnetic bearing (SMB) with a central superconductor. A central superconductor improves stiffness of each direction. In addition, characteristics of magnetically levitated superconducting conveyor are studied when the levitated table moves in the y direction.

1 Introduction

In semiconductor manufacturing industry, various kinds of machines with mechanical contacts are used in vacuum chambers. In general, oil-free mechanical bearings such as journal bearings and ball bearing useful in vacuum environments are applied to the semiconductor industry. However, mechanical bearings produce small dusts in vacuum environments. On the other hand, magnetic levitation technologies give us several advantages [1-3]. Our group has made a magnetically levitated conveyor using superconducting magnetic bearings (SMBs) [4]. Vibrations of the conveyor are suppressed by using forces between coils and permanent magnets (PMs). Repulsion magnet is effective in improving of levitation height and improving forces in the z direction [5]. However, it could not improve forces in the x and y directions. Thus, a new structure to get larger levitation forces compared with the previous conveyers is proposed. The new conveyor has SMBs with a high temperature superconductor (HTSC) in the center. Moreover, two types of PMs are discussed to improve levitation forces.

2 System

A block diagram of a magnetically levitated conveyor system is shown in Figure 1. The conveyor is composed of a magnetically levitated table and a conveying table. The conveyor is composed of two SMBs. Each SMB consists of a levitated PM and a bulk HTSC. Under each HTSC, there is a coil to suppress table vibrations by using control technique. An initial gap between levitated table and conveying table is set using field-cooling method. The superconductors are field-cooled to a temperature lower than a critical temperature (T_c). The levitated table moves following the conveying table due to flux pinning forces. Signals of table displacement are put into a personal computer (PC) through A/D converters. Control signals from D/A converters are put into power amplifiers. Then, left and right coils are excited to suppress the table vibrations by using PD control.

*komori_mk@yahoo.co.jp, Department of Applied Science for Integrated System Engineering, Kyushu Institute of Technology, 1-1 Sensui, Tobata, Kitakyushu, Fukuoka 804-8550, Japan, Phone/Fax +81-93-884-3563

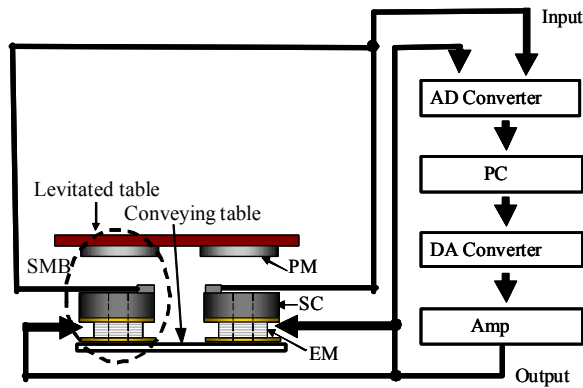


Fig. 1. Block diagram of a magnetically levitated conveyor system.

3 SMB Structures

3.1 Structure of SMB

In magnetic levitations, levitation forces are affected by the magnetic field in the radial direction. Then, two types of SMBs with a central superconductor are studied as shown in Figure 2. Figure 2(a) shows a SMB composed of a doughnut-shaped superconductor ($\approx \phi 49 \text{ mm} \times \phi 24 \text{ mm} \times 25 \text{ mm}$), a cylindrical superconductor ($\phi 9.0 \text{ mm} \times 25 \text{ mm}$) in the center of the doughnut-shaped superconductor, a levitated disk-shaped PM ($\phi 30 \text{ mm} \times 5 \text{ mm}$, surface magnetic flux density: 0.3 T) and an electromagnet (EM) under the disk-shaped superconductor, corresponding to type-1 SMB. The cylindrical superconductor is used for levitation and for making magnetic flux path between two superconductors. The levitated PM in Figure 2(b) is a doughnut-shaped PM ($\phi 30 \text{ mm} \times \phi 14 \text{ mm} \times 5 \text{ mm}$, surface magnetic flux density: 0.3 T), corresponding to type-2 SMB. Table 1 shows the lists of these parameters.

Figure 3 shows the magnetic flux density distributions in the radial direction of the type-1 and type-2 SMBs. The magnetic flux density is measured on the surface of PMs. In the case of type-1 SMB, magnetic flux density distribution shows a point symmetry around the center of PM. In the case of type-2 SMB, there is a doughnut-shaped magnetic flux distribution as shown in Figure 3(b). The gradient of magnetic flux density is expected to improve the levitation force of type-2 SMB shown in Figure 2(b).

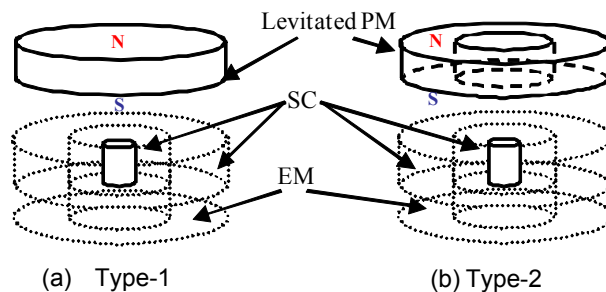


Fig. 2. SMB structures of (a) type-1 and (b) type-2.

Table. 1 Lists of Parameters.

Superconductor (L side)	f 48.7 × f 23.7mm, $Y_1B_{a2}Cu_3Ox$, $J_c \sim 1 \times 10^8 A/m^2$ at 1T, 77K
Superconductor (R side)	f 49.4 × f 25.7mm, $Y_1B_{a2}Cu_3Ox$, $J_c \sim 1 \times 10^8 A/m^2$ at 1T, 77K
Electric Magnet (L side)	f 86 × 48mm 900 turns
Electric Magnet (R side)	f 87 × 48mm 900 turns
Levitation Magnet	f 30 × 5mm, Mass: 25g
Levitation Magnet (ring type)	f 30 × f 14 × f 5mm, Mass: 20g
Levitated stage	Mass: 90g (ring type)

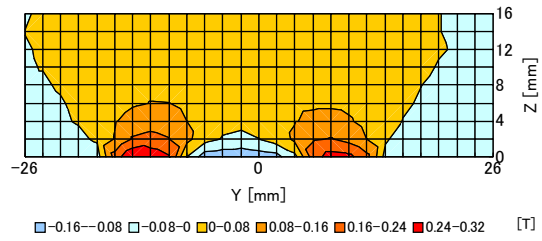
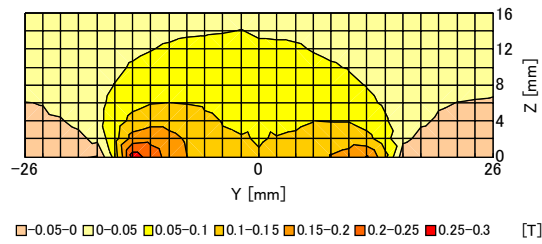


Fig.3. Magnetic flux density distributions of levitation magnets of (a) type-1 PM and (b) type-2 PM.

3.2 Static characteristics of type-2 SMB

Figure 4 shows an experimental setup for measuring repulsion forces between HTSC and PM. In the measurement, a z-stage and a load cell are connected to the levitated PM. The attraction and repulsion forces are measured by using the load cell for various applied currents from -1.0 A to 1.0 A. Figure 5 shows the relationships between attraction/repulsion force and applied current, representing the force (a) in the y direction and (b) in the z direction.

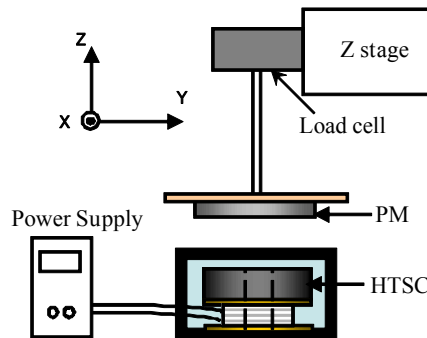


Fig. 4 Experimental setup for repulsion forces between PM and HTSC.

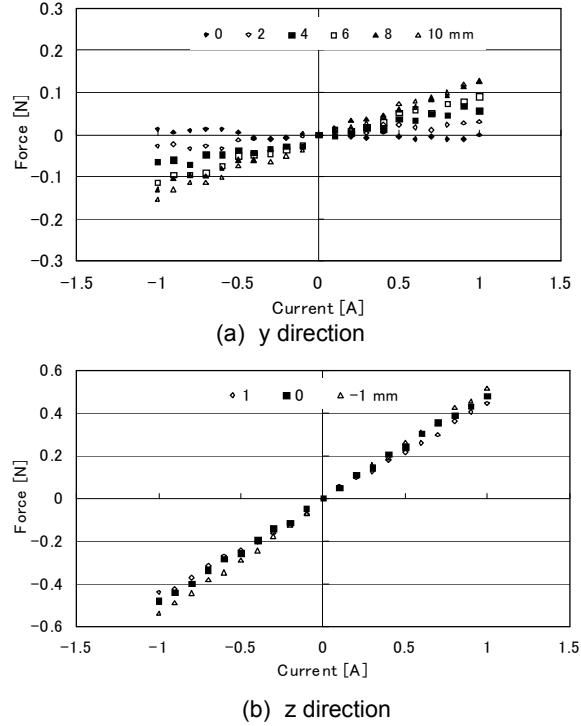


Fig. 5 Relationships between attraction/repulsion force and applied current.

The repulsion force and attraction force show minus sign and plus sign, respectively. Since field-cooling is performed at a distance of 12 mm, the levitation force at the distance is 0 N. Figures 5 (a) and (b) show the linear relationships between force and applied current. The gradients of y and z directions are 0.07 N/A (4 mm) and 0.49 N/A, respectively. The gradients of x and y directions are almost the same, because the magnetic flux distribution shows a point symmetry. As a result, the attraction and repulsion forces of x and y directions are improved.

4 Experiments and Discussions

4.1 Impulse response of SMB

Impulse responses of type-1 SMB and type-2 SMB in the y direction are measured. Impulses are applied to the levitated PM in the y direction. The displacement is measured by using a laser displacement sensor. The initial gap between levitated PM and HTSC is 12mm. The vibration in Figure 6(a) disappears within several seconds. On the other hand, the vibration in Figure 6(b) disappears within ≈ 1.5 s, which is about one-second of Figure 6(a). The experimental results show that the damping coefficient of type-2 SMB is larger than that of type-1 SMB. This is because the gradient of magnetic flux density in Figure 3(b) is larger than that in Figure 3(a). That is, the type-2 SMB is more effective than the type-1 SMB.

Hereafter, the type-2 SMB is adopted for the magnetically levitated conveyer.

4.2 Impulse response of two-axis control

Our group applied the type-2 SMB (Figure 3(b)) to the magnetically levitated conveyer. Then, the levitated table is supported by two type-2 SMBs as shown in Figure 7. Xyz coordinate is indicated in Figure 7. Impulse responses of the magnetically levitated table are studied.

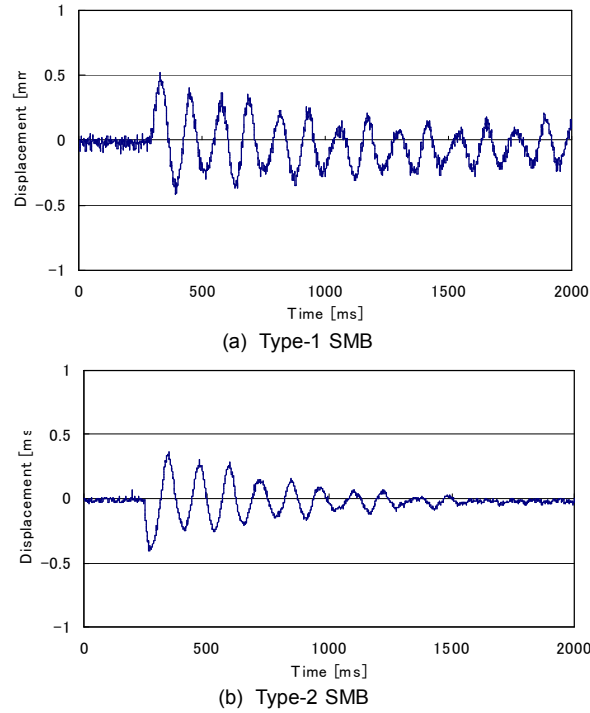


Fig. 6. Impulse responses of (a) type-1 SMB and (b) type-2 SMB

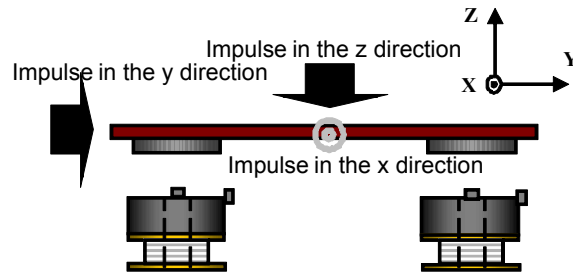


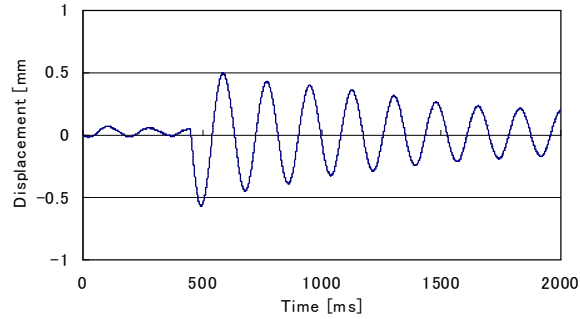
Fig. 7. Experimental setup of impulse responses in the x, y and z directions

Impulse responses in the x direction are studied using the experimental setup shown in Figure 7. In the experiments, impulses are applied to the levitated table. Then, the displacement of the levitated table in the x direction is measured. The displacement is measured by using a laser displacement sensor. Figure 8 shows the experimental result of impulse responses in the x direction (a) without control and (b) with control. The vibration in Figure 8(a) disappears within a few seconds. On the other hand, the vibration in Figure 8(b) disappears within ≈ 1 s. However, the vibrations are not well suppressed as shown in Figure 8 in spite of PD control. This is because other vibration modes are added to the vibration in the x direction.

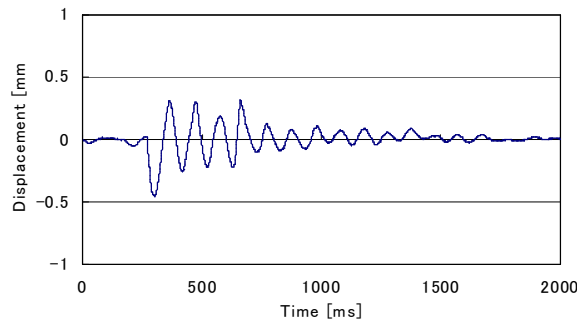
Impulse responses in the y direction are studied using the experimental setup shown in Figure 7. Figure 9 shows the experimental result of impulse response in the y direction (a) without control and (b) with control. The vibration in Figure 9(a) disappears within a few seconds. On the other hand, the vibration in Figure 9(b) disappears within ≈ 0.5 s. The vibrations are well suppressed by using PD control as shown in Figure 9(b).

Impulse responses in the z direction are studied using the experimental setup shown in Figure 7. Figure 10 shows the experimental result of impulse response in the z direction without control, showing (a) the central displacement and (b) the rotation angle in the center of table. Both vibrations in Figures 10(a) and (b) disappear within a few seconds. Figure 11 shows the experimental result of impulse responses in the z direction with control, showing (a) the central displacement and (b) the rotation angle in the center of table. Both vibrations in Figures 11(a) and

(b) disappear within ≈ 0.5 s, which are about one-fourth of the vibration time in Figure 10. Figure 11 shows that the vibrations of the levitated table are well suppressed by using PD control.

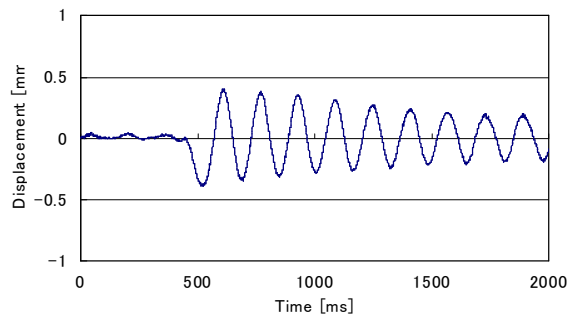


(a) Without control

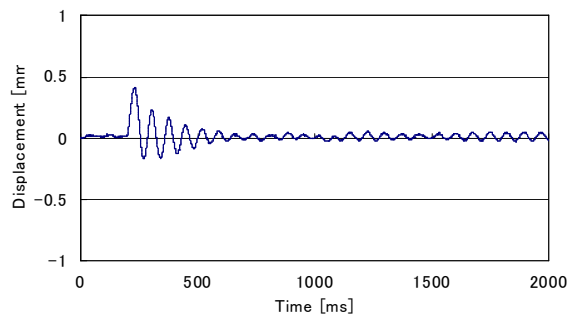


(b) With control

Fig. 8. Impulse responses in the x direction (a) without control and (b) with control.

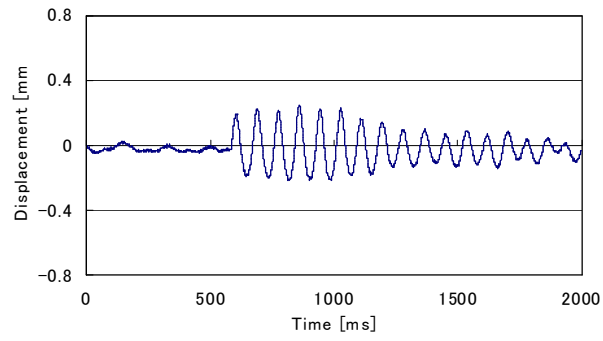


(a) Without control

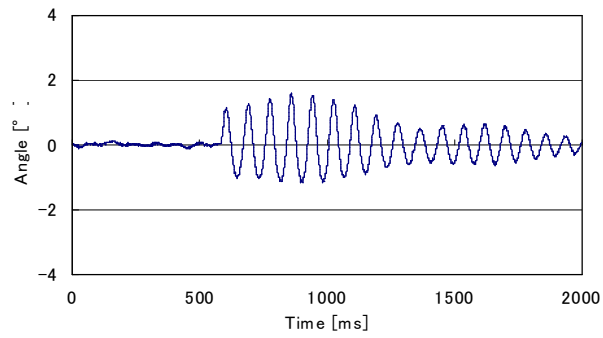


(b) With control

Fig. 9. Impulse responses in the y direction (a) without control and (b) with control.

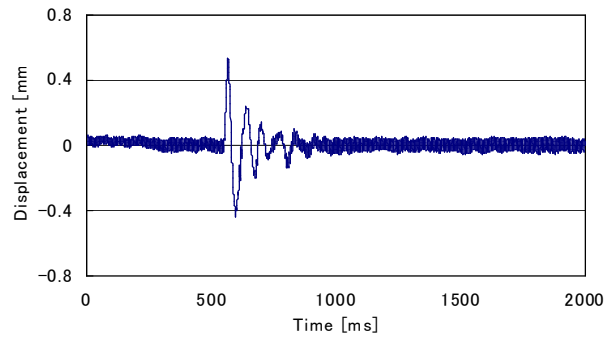


(a) Central displacement

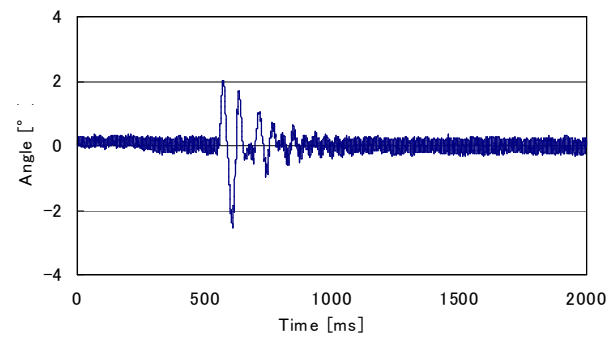


(b) Angle

Fig. 10. Impulse responses in the z direction without control.



(a) Central displacement



(b) Angle

Fig. 11. Impulse response of the z direction with control

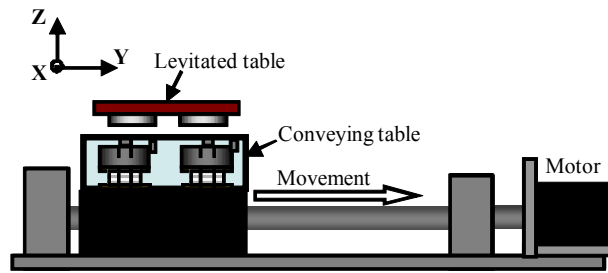
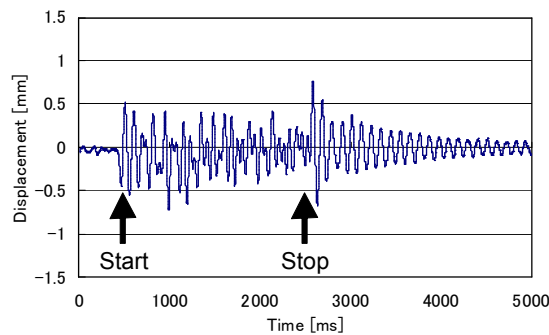


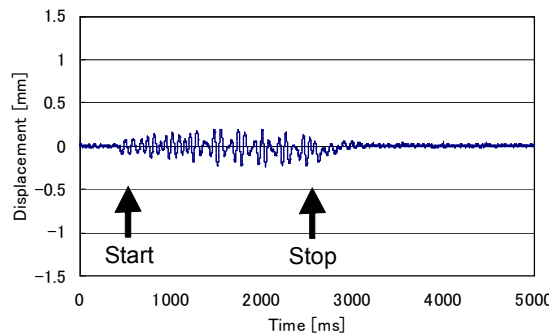
Fig. 12. Setup of conveying experiments for the magnetically levitated conveyor

4.3 Conveying experiments

Figure 12 shows the setup of conveying experiments for the magnetically levitated superconducting conveyor. The superconductors are set in the container (conveying table) filled with liquid nitrogen. The initial gap between levitated table and conveying table is 12 mm. Characteristics of magnetically levitated superconducting conveyor are studied when the levitated table moves in the y direction. Then, the displacement is measured by using Hall sensors. Figure 13 shows the relationships between table displacement in the x direction and time (a) without control and (b) with control. In Figure 13, the magnetically levitated conveyor starts at ≈ 0.5 s and stops at ≈ 2.5 s. In comparison with Figure 13(a) and (b), the displacements in Figure 13(b) are smaller than those in Figure 13(a). However, the displacements of levitated table are not well suppressed by using PD control as shown in Figure 13(b). This is because vibrations in the y and z directions occur after impulses are applied to the table in the x direction. Figure 14 shows the relationships between table displacement in the y direction and time (a) without control and (b) with



(a) Without control



(b) With control

Fig. 13. Relationships between table displacement in the x direction and time (a) without control and (b) with control.

control. In the case without control in Figure 14(a), the displacements of levitated table show 0.3 mm, and show 0.4 mm just after the conveyer stops at ≈ 2.5 s. In the case with control in Figure 14(b), the vibrations of levitated table are suppressed in the range smaller than 0.1 mm after the conveyer starts at ≈ 0.5 s and stops at ≈ 2.5 s. Figure 15 shows the relationships between table displacement in the z direction and time (a) without control and (b) with

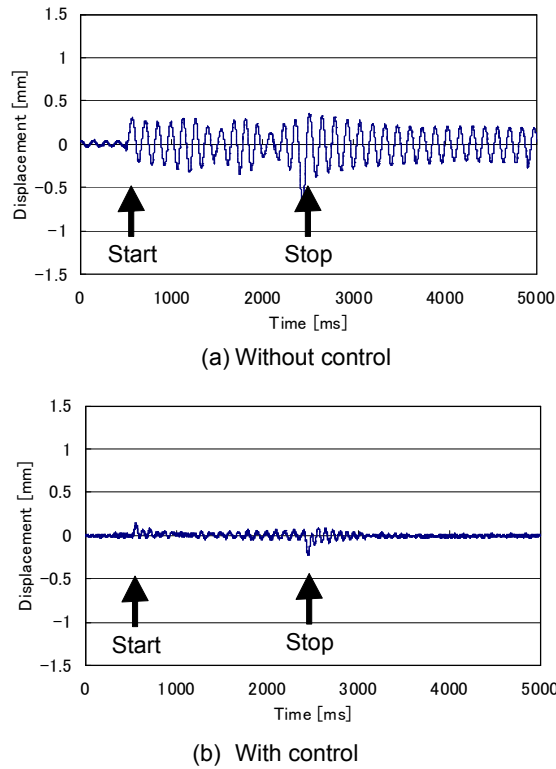
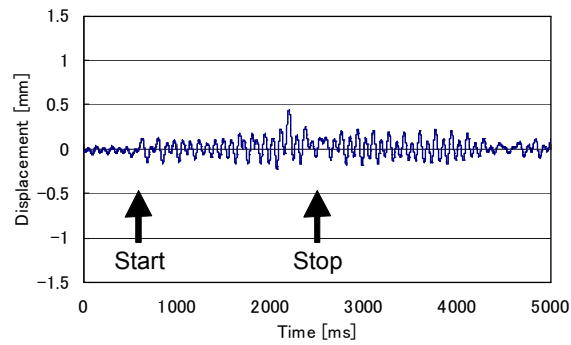


Fig. 14. Relationships between table displacement in the y direction and time (a) without control and (b) with control.

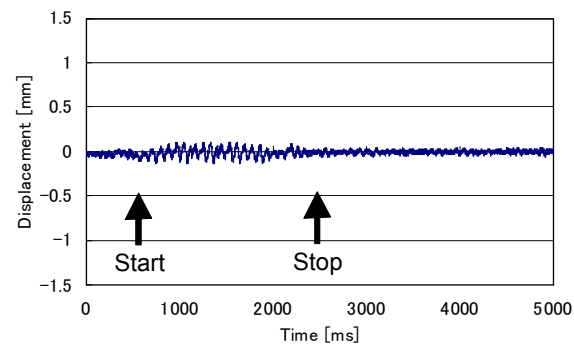
control. In the case without control in Figure 15(a), the displacement of levitated table shows 0.3 mm just after the conveyer starts, and the displacement shows 0.4mm just after the conveyer stops. In the case with control in Figure 15(b), the vibrations of levitated table are suppressed in the range smaller than 0.1 mm after the conveyer starts and stops.

5 Summary

This paper discusses the improvement of magnetically levitated superconducting conveyer. A SMB with a central superconductor is proposed. The static and dynamic characteristics of the SMB are studied. From the experimental results, it is found that the type-2 SMB composed of doughnut-shaped PM is useful to the conveyer. Characteristics of the magnetically levitated superconducting conveyer are studied. The experimental results of impulse responses show that the vibrations of levitated table disappear within ≈ 0.5 s by using PD control. These show that the vibrations are suppressed well by using PD control in the x, y and z directions.



(a) Without control



(b) With control

Fig. 15. Relationships between table displacement in the z direction and time (a) without control and (b) with control.

References

- [1] Kojima H., Itagaki O., Okabe T. and Kobayashi T., *J. of Robotics Society of Japan*, 14, 868, 1996.
- [2] Ohashi S. and Dodo D., *IEEE Trans. on Applied Superconductivity*, 17(2), 2083, June 2007.
- [3] Kudou Y., Ueda H. and Ishiyama A., *IEEE Trans. Applied Superconductivity*, 15(2), 2230, June 2005.
- [4] Mori T. and Komori M., *IEEE Trans. on Applied Superconductivity*, 17(2), 2170, June 2007.
- [5] Uchiyama T., Nakaya B., Inoue A and Komori M., *IEEE Trans. on Applied Superconductivity*, 19(3), 2107, June 2009.